Molecular Crystals and Liquid Crystals

Publication details, including instructions for authors and subscription information:
http://www.tandfonline.com/loi/gmcl20

Two-Wave Coupling during the Formation of POLICRYPS Diffraction Gratings: Experimental Results Theoretical Model

A. Veltri [a] , R. Caputo [a] , L. De Sio [a] , C. Umeton [a] & A. V. Sukhov [b]

[a] Liquid Crystal Laboratory - LICRYL, National Institute for the Physics of Matter of the National Council of Researches (INFM-CNR), Centro di Eccellenza per Materiali Innovativi Funzionali in Calabria-CEMIF.CAL and Department of Physics, University of Calabria, Rende, (CS), Italy

[b] Institute for Problems in Mechanics, Russian Academy of Science, Moscow, Russia

Version of record first published: 22 Sep 2006

To cite this article: A. Veltri, R. Caputo, L. De Sio, C. Umeton & A. V. Sukhov (2006): Two-Wave Coupling during the Formation of POLICRYPS Diffraction Gratings: Experimental Results Theoretical Model, Molecular Crystals and Liquid Crystals, 454:1, 273/[675]-284/[686]

To link to this article: http://dx.doi.org/10.1080/15421400600656426

Mol. Cryst. Liq. Cryst., Vol. 454, pp. 273/[675]–284/[686], 2006

ISSN: 1542-1406 print/1563-5287 online
DOI: 10.1080/15421400600656426

Taylor & Francis
Taylor & Francis Group

Two-Wave Coupling during the Formation of POLICRYPS Diffraction Gratings: Experimental Results Theoretical Model

A. Veltri
R. Caputo
L. De Sio
C. Umeton
Liquid Crystal Laboratory – LICRYL, National Institute for the Physics of Matter of the National Council of Researches (INFM-CNR), Centro di Eccellenza per Materiali Innovativi Funzionali in Calabria-CEMIF.CAL and Department of Physics – University of Calabria, Rende (CS), Italy

A. V. Sukhov
Institute for Problems in Mechanics, Russian Academy of Science, Moscow, Russia

In this paper we report the investigation of a beam coupling effect that occurs during the formation (by UV curing) of POLICRYPS diffraction gratings. Along with observations, we present a complete theoretical model which accounts for the main experimental features of the effect. Numerical solutions confirm the observed absence of any energy transfer process for unit ratio of the impinging beam intensities. When this ratio is not unit, the transfer is instead present and tends to equalize the beam intensities during the curing process; the capability of performing this equalization is strongly related to the grating diffraction efficiency. Furthermore, in this case, numerical simulations enable also to visualize the final (distorted) morphology of the fabricated structure.

Keywords: diffraction gratings; liquid crystals; polymers

Address correspondence to C. Umeton, Liquid Crystal Laboratory – LICRYL, National Institute for the Physics of Matter of the National Council of Researches (INFM-CNR), Centro di Eccellenza per Materiali Innovativi Funzionali in Calabria-CEMIF.CAL and Department of Physics – University of Calabria, I-87036 Rende (CS), Italy.

INTRODUCTION

In the last decades, realization and investigation of diffraction gratings in liquid crystalline composite materials have attracted great attention. In particular, Holographically formed Polymer Dispersed Liquid Crystals (HPDLC) [1,2] and POlymer LIquid CRYstal Polymer Slices (POLICRYPS) [3,4] holographic gratings have been investigated also for their application oriented aspects, which involve light control [5,6], holographic recording [7,8] and display technology [9–11]; in these applications, the overall performances of obtained gratings play a fundamental role. If gratings are fabricated by using a visible or UV interference pattern for curing a monomer-liquid crystal pre-syrup, the quality of samples can be strongly affected by occurrence of an energy exchange between the interfering beams. Their modification inside the sample during the curing process leads to the formation of gratings with tilted or curved fringes and such deformations affect the fundamental optical and electro–optical features of the grating. These wave mixing effects, firstly observed in HPDLC formation [12,13], proved to occur also during the fabrication of POLICRYPS gratings [14].

In this paper we report on the main features of the two wave mixing effect that can occur during the formation of POLICRYPS gratings, along with a general theoretical model implemented to explain these features. Furthermore, this model enables to visualize the morphology of the fabricated grating.

EXPERIMENT

If we couple two interfering plane waves by means of a transmission Bragg grating which has the same periodicity of their interference pattern, the fields $E_{1,2}(L)$ at the exit of the grating can be written as:

$$\begin{cases} E_1(L) = i\exp(-i\varphi_L)E_2^{in}\sqrt{\eta} + E_1^{in}\sqrt{1-\eta} \\ E_2(L) = i\exp(i\varphi_L)E_1^{in}\sqrt{\eta} + E_2^{in}\sqrt{1-\eta} \end{cases} \tag{1}$$

were $E_{1,2}^{in}$ represent the electric amplitudes of the curing waves at the entrance of the grating; η is the (time dependent) diffraction efficiency and φ_L is an additional phase shift of the cured grating with respect to the interference pattern, which can be due to several, different, effects. From (1), the value of the ratio between the intensities $\mathrm{I}_1(L), \mathrm{I}_2(L)$ of the outgoing beams can be calculated as:

$$R(L) = \frac{\mathrm{I}_1(L)}{\mathrm{I}_2(L)} = \frac{\eta + (1-\eta)R_0 + 2\sin(\varphi_L)\sqrt{R_0\eta(1-\eta)}}{\eta R_0 + (1-\eta) - 2\sin(\varphi_L)\sqrt{R_0\eta(1-\eta)}} \tag{2}$$

where R_0 is the intensity ratio at the entrance of the grating. Since expression (2) indicates that, through φ_L, also setup instabilities can be responsible for an induced phase shift, we designed an *in situ* control system that allows a monitoring of the stability of the setup, shown in Figure 1.

This is the one used for curing POLICRYPS gratings [3], modified by mounting a commercial metal-coated reflective diffraction grating on the same steel disk which holds the sample. This reference grating (see insertion in Fig. 1) is vertically separated by a 3 mm distance from the sample aperture; in this way, it reflects and contemporarily diffracts the peripheral parts of the impinging (15 mm-broad) beams. Their angle of intersection is set in such a way that the reflected part of one of them spatially coincides with the diffracted part of the second one. The combined diffracted/reflected outgoing beam is spatially separated from the incident one (by a slight vertical misalignment of the reference grating) and then detected by a third photodiode PD_3 placed above one of the two mirrors of the interferometer. Thus, the intensity registered by PD_3 turns out to be:

$$I_{ref} = I_1 + I_2 + 2\sqrt{I_1 I_2}\sin\varphi_{ref} \tag{3}$$

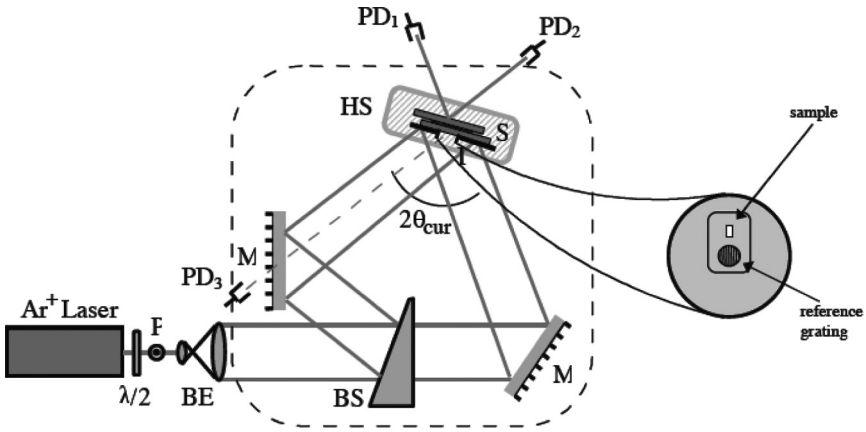

FIGURE 1 Optical setup for UV curing of POLICRYPS gratings and contemporary stability check. P, polarizer; $\lambda/2$, half-wave plate; BE, beam expander; BS, beam splitter; 2θcur, total curing angle; M, mirrors; HS, hot stage; I, tuneable aperture; S, sample; PD1, first beam photo-detector; PD2, second beam photo-detector; PD3, diffracted/reflected beam photo-detector. In the insertion it is shown the reference grating, put below the sample, used for the stability check.

where $I_{1,2}$ are the intensities of the reflected part of the first beam and the diffracted part of the second one respectively, and φ_{ref} is the phase shift between the reference grating and the curing interference pattern. In order to reduce all sources of vibration, reinforced posts and mounts are adopted, while the interferometric part of the set-up is placed on a thick steel plate and covered with a hermetic box made of sound absorbing, thermo isolating material. For this setup, typical values of the phase shift introduced by vibrations (measured by means of Eq. (3)) does not exceed ± 4–5°, which represents the limiting accuracy of our experiment.

For the sample preparation, we utilize 5CB nematic liquid crystal diluted in NOA-61 Norland Optical Adhesive. Sample cells, with a nematic concentration below 30%, by weight, are made by using Indium Tin Oxide (ITO)–coated glass slabs and have a $L = 15\,\mu m$ thickness. Gratings are cured at room temperature by illumination with the interference pattern formed by two laser beams at $\lambda_B = 351\,nm$. The total impinging intensity is maintained constant at $I_0 = 4,1\,mW/cm^2$, this value being optimal from the viewpoint of the final diffraction efficiency [3]. The fringe spacing of the interference pattern is $\Lambda = 0,417\,\mu m$, corresponding to a pronounced Bragg regime ($\rho = 2\lambda_B^2/\Lambda^2\epsilon_1 \approx 110$) [15].

RESULTS

Experimental results strongly depended on the value of R_0: With $R_0 = 1$, no beam coupling is observed (Fig. 2). For $R_0 \neq 1$, the wave mixing takes place and tends to equalize the intensities of the two curing beams inside the sample. The effect, well pronounced for $R_0 \approx 0.5$, becomes weaker for $R_0 \leq 0,3$. It is worth noting that all beam coupling effects take place in the very beginning of the curing process, when diffusion processes are noticeable [16]. Finally, the real additional phase shift of the diffracted waves, given by $\varphi_{L1}(t) = (\varphi_L(t) - \varphi_{ref}(t) + \varphi_{ref}(t=0))$, is reported in Figure 3, for two different values of R_0: Figure 1. Figure 1(a) represents the switching curve of the POLICRYPS grating.

It is evident that $\varphi_{L1}(t)$ increases with increasing deviation of R_0 from its unit value. In conclusion of this section, we can state that the observed two wave coupling effect exhibits the following features:

- It depends on the phase shift between the impinging interference pattern and the grating that is being cured;
- It does not take place if the two interfering beams have the same intensity;

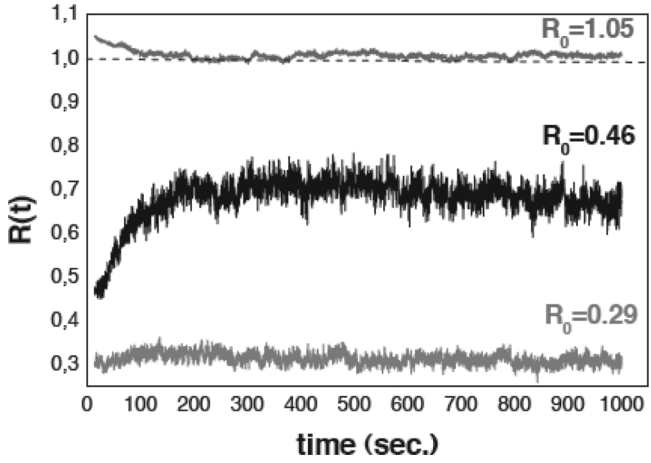

FIGURE 2 Temporal behavior of the intensity ratio of the two beams, used to cure the POLICRYPS, transmitted through the sample. No energy transfer takes place in case of initial unit ratio of the beams.

- If the initial ratio R_0 of the beam intensities is different from the unit value, the beam coupling takes place and tends to equalize the intensities of the beams outgoing from the grating;
- When it occurs, the effect is the weaker the further R_0 deviates from the unit value;

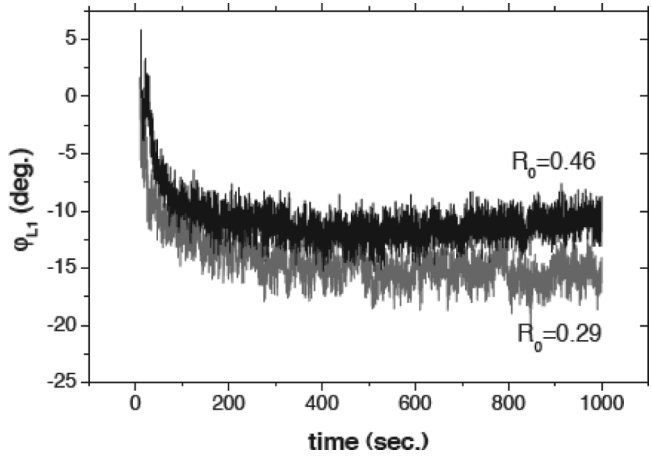

FIGURE 3 Phase shift of the diffracted waves, in case of stable interference pattern, for different initial ratio of the two impinging intensities.

- The diffraction efficiency of the fabricated grating decreases with the deviation of R_0 from the unit value;
- The additional phase shift of a probe light wave diffracted by the cured grating increases with the deviation of R_0 from the unit value.

THEORETICAL MODEL

Starting from the experimental evidence, in a previous paper [17] we have reported an approximate theoretical model. First of all, we have excluded a photorefractive origin of the observed phenomenon. In our case, indeed, measurements of sample conductivity showed a negligible presence of free charge carriers before the curing process started, and no variation after curing. We have then coupled the system of Helmholtz equations, which describe the spatial evolution of the curing beams inside the sample, to a material equation that, in order to depict the grating formation in the medium stated that the rate of the first spatial Fourier component of the optical permittivity is proportional to the intensity of the curing interference pattern. Approximate analytical solutions of the obtained system, although enabling to satisfactory explain all observed features, were limited to predict the occurrence of the wave mixing effect. In this paper, we present a new, non approximated, theoretical approach which consists in coupling the Helmholtz equations for light propagation in periodic media to a detailed chemical diffusive model for the grating formation in liquid crystalline composite materials [18]. We start by writing the Helmholtz equations:

$$\frac{\partial \boldsymbol{E}_1}{\partial \zeta} = \frac{2\pi i}{\Lambda \lambda_B \cos\beta} \boldsymbol{F}_1^*[\epsilon(\xi)]\boldsymbol{E}_2 \tag{4}$$

$$\frac{\partial \boldsymbol{E}_2}{\partial \zeta} = \frac{2\pi i}{\Lambda \lambda_B \cos\beta} \boldsymbol{F}_1[\epsilon(\xi)]\boldsymbol{E}_1$$

Here i is the imaginary unit; ζ and ξ are the normalized coordinates for the z and x axes respectively, namely $\zeta = \mathrm{q}z$, $\xi = \mathrm{q}x$, where $\mathrm{q} = 2\pi/\Lambda$ is the grating vector; λ_B is the wavelength of the curing radiation; β the refraction angle of the curing beams inside the medium; $\boldsymbol{F}_1[\epsilon(\xi)]$ stands for the first component of the Fourier transform of the dielectric constant across the grating $\boldsymbol{F}_1^*[\epsilon(\xi)]$ being its complex conjugate. $\epsilon(\xi)$ is the profile for the dielectric constant of the medium; in our sample.

$$\epsilon(\xi) = \epsilon_N \sigma(\xi) + \epsilon_P(\nu(\xi) + \mu(\xi)) \tag{5}$$

where $\sigma(\xi) = C/T$, $\nu(\xi) = P/T$ and $\mu(\xi) = M/T$ are the normalized concentrations of liquid crystals (C), polymers (P) and monomers (M) respectively (T stands for the total molecular concentration), so that

$$\sigma(\xi) + \nu(\xi) + \mu(\xi) = 1; \tag{6}$$

Furthermore, were we have assumed that the dielectric constant of polymer and monomer is the same and it is ϵ_{P}; for the liquid crystal dielectric constant we have used

$$\epsilon_N = \left(\frac{2n_o + n_e}{3}\right)^{1/2}$$

where n_o and n_e are respectively the ordinary and the extraordinary refractive indices of the nematic liquid crystal. Taking into account Eq. (6), expression (5) becomes:

$$\epsilon(\xi) = \epsilon_N \sigma(\xi) + \epsilon_P(1 - \sigma(\xi))$$

and finally we get

$$\epsilon(\xi) = \Delta\epsilon\sigma(\xi) + \epsilon_P \tag{7}$$

where $\Delta\epsilon = \epsilon_{\mathrm{P}} - \epsilon$. In this way,

$$F_1[\epsilon(\xi)] = \Delta\epsilon F_1[(\sigma(\xi))] \tag{8}$$

The system of coupled equations that govern the whole process is therefore given by

$$\frac{d\mu(\xi,\zeta,\tau)}{d\tau} = B\frac{\partial}{\partial\xi}\left[(1-\nu)^{2/3}\frac{\partial}{\partial\xi}\left(\frac{\mu}{1-\nu}\right)\right] - W^{1/2}\mu \tag{9}$$

$$\frac{d\nu(\xi,\zeta,\tau)}{d\tau} = \frac{G}{2}W\left[N_0^2(1-\gamma) + N_0(1+\gamma) + \frac{2\gamma}{1-\gamma}\right]\gamma^{N_0} \tag{10}$$

$$\frac{d\sigma(\xi,\zeta,\tau)}{d\tau} = B\frac{\partial}{\partial\xi}\left[(1-\nu)^{2/3}\frac{\partial}{\partial\xi}\left(\frac{\sigma}{1-\nu}\right)\right] \tag{11}$$

$$\frac{\partial E_1(\zeta,\tau)}{\partial\zeta} = \frac{2\pi i\Delta\epsilon}{\Lambda\lambda_B\cos\beta}F_1^*[\sigma]_\xi E_2 \tag{12}$$

$$\frac{\partial E_2(\zeta,\tau)}{\partial\zeta} = \frac{2\pi i\Delta\epsilon}{\Lambda\lambda_B\cos\beta}F_1[\sigma]_\xi E_1 \tag{13}$$

$$W(\xi,\zeta,\tau)=\frac{1}{2}\left(1+\frac{E_1(\zeta,\tau)E_2(\zeta,\tau)^* e^{i\xi}+E_1^* E_2 e^{i\xi}}{E_1E_1^*+E_2E_2^*}\right) \tag{14}$$

where N_0 stands for the least number of monomer molecules which are needed for the formation of an immobile polymer chain. Furthermore, we have introduced a dimensionless time

$$\tau=[k_p/k_t(k_t g\,WI)^{1/2}]t$$

and parameters B, G and γ defined as:

$$B=\frac{4\pi D k_t^{1/2}}{(gW_0I)^{1/2}\Lambda^2}=G\frac{(gW_0Ik_t)^{1/2}}{k_pT}.$$

$$\gamma=\frac{\mu}{\mu+G\sqrt{(1+m\sin\xi)}}$$

where t is the time, I is the initiator concentration, k_p and k_t are the chemical prolongation and termination constants for the polymer formation reactions, g represents the activation probability of the initiator molecules when acted on by the radiation; D is the monomer diffusion constant; $W_0=I_1+I_2$ with $I_1=E_1\,E_1^*$ and $I_2=E_2\,E_2^*$ intensities of the two interfering beams; $m=2(\sqrt{I_1I_2}/(I_1+I_2))$ is the visibility of the fringes.

NUMERICAL SOLUTIONS

Equations (9)–(14) represent a time dependent, spatially 2D system; to solve it, we have implemented a central derivative scheme for Eqs. (12) and (13) concerning light propagation and we have coupled them to the numerical scheme described elsewhere [16]. Our code can display now the time evolution of diffraction efficiency during curing, the time evolution of the intensity of both curing beams as well as the morphology of the forming grating. First of all we have realized the theoretical equivalent of Figure 2, by choosing $B=1$ and $G=0.2$, which correspond to the experimental situation presented in Ref. 14. Results of this characterization are presented in figure 4.

It is possible to see that the model confirms the experimentally observed absence of energy transfer process for unit ratio of the impinging beam intensities. When this ratio is not unit, the transfer is instead present and tends to equalize the beam intensities during the curing process. The advantage of available numerical solutions

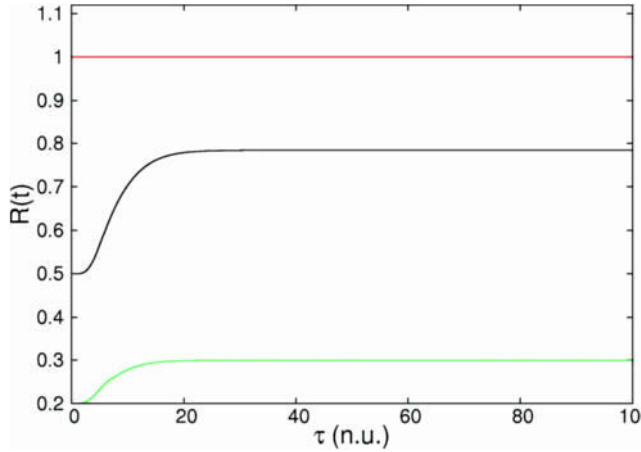

FIGURE 4 Numerical simulation of the temporal behavior of the intensity ratio of the curing beams, transmitted through the sample. Again there is no energy transfer in the case of initial unit ratio of the beams.

is also the possibility of verifying the final morphology of the realized grating. In this way it is possible to appreciate the consequences of the investigated phenomena on the morphology of the fabricated structure. The calculated difference is dramatic: with an initial beam ratio different from unity, an energy transfer effect occurs, which produces a weaker grating with slanted fringes, as the one shown in Figure 5(b).

The energy transfer, which is present for $R_0 \neq 1$, tends to equalize the beam intensities during the curing process; moreover the capability of the system to equalize the beam intensities is strongly related to its diffraction efficiency: the higher is the diffraction efficiency, the better will be the realized equalization of the beam intensities. In Figure 6 it is presented the Final Diffraction Efficiency of the produced grating calculated as a function of the initial intensity ratio of the curing beams R_0. It is possible to appreciate that, like experimental values reported in Figure 7, the final diffraction efficiency (DE) decrease drastically when the beams are unbalanced and the beam exchange process takes place.

In conclusion, we have presented the observation of a beam coupling effect occurring during the UV curing of POLICRYPS diffraction gratings, along with a complete theoretical model which accounts for the main features of this effect. The model confirms the experimentally observed absence of an energy transfer process for unit ratio

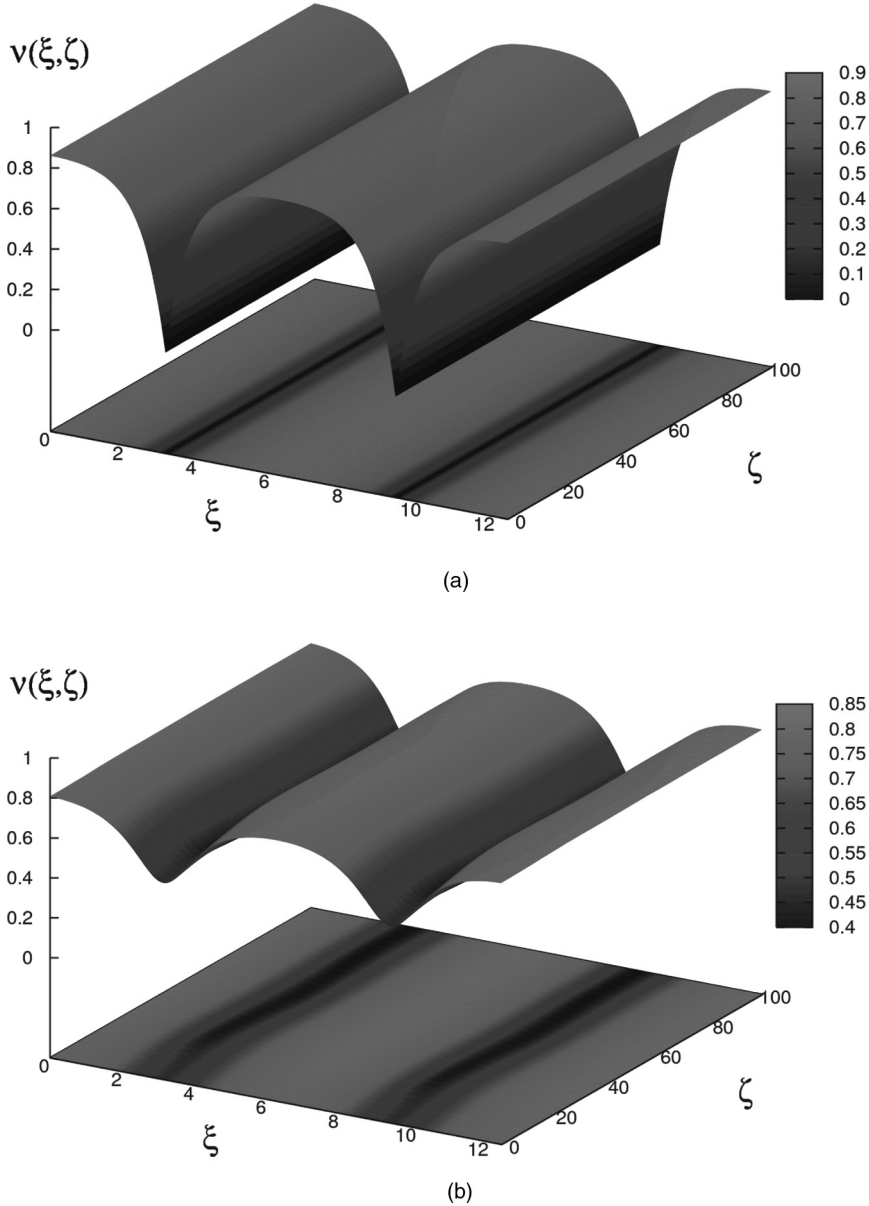

FIGURE 5 Numerical simulation for the behavior of polymer concentration $\nu(\xi, \zeta)$ as a function of the normalized spatial coordinates ξ and ζ when the curing process can be considered completed; (a) corresponds to $R_0 = 1$, while (b) corresponds to $R_0 = 1/2$.

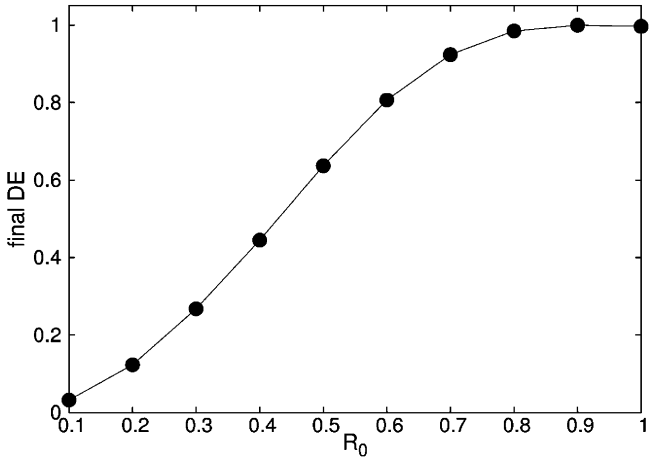

FIGURE 6 Numerical Simulation of the dependence of the steady state value of the diffraction efficiency versus the initial intensity ratio of the curing beams.

of the impinging beam intensities. When this ratio is not unit, the transfer is instead present and tends to equalize the beam intensities during the curing process; in this case, the model enables also to visualize the distorted morphology of the fabricated structure. The capability of performing the above mentioned equalization is strongly related to the grating diffraction efficiency: the higher it is, the better the equalization of the outgoing beam intensities is realized.

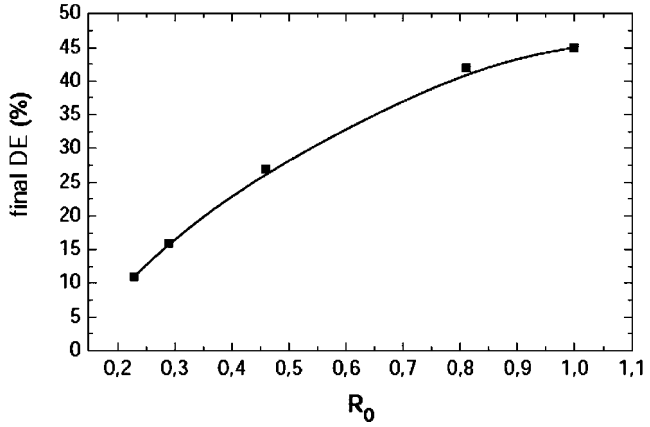

FIGURE 7 Experimental dependence of the final value of the diffraction efficiency on the initial intensity ratio of the curing beams.

REFERENCES

[1] Sutherland, R. L., Tondiglia, V. P., Natarajan, L. V., Bunning, T. J., & Adams, W. W. (1996). Electro-optical switching characteristics of volume holograms in polymer dispersed liquid crystals. *J. Nonlinear Opt. Phys. & Materials*, *5*, 89.

[2] Lucchetta, D. E., Karapinar, R., Manni, A., & Simoni, F. (2002). Phase-only modulation by nanosized polymer-dispersed liquid crystals. *J. Appl. Phys.*, *91*, 6060.

[3] Caputo, R., De Sio, L., Sukhov, A. V., Veltri, A., & Umeton, C. (2004). Development of a new kind of holographic grating made of liquid crystal films separated by slices of polymeric material. *Opt. Lett.*, *29*, 1261.

[4] Caputo, R., Sukhov, A. V., Umeton, C., & Veltri, A. (2004). Characterization of the diffraction efficiency of new holographic gratings with a nematic film-polymer slice sequence structure (POLICRYPS). *Journal of Optical Society of America B*, *21*, 1939.

[5] Fuh, A. Y.-G., Huang, C.-Y., & Tzen, B.-W. (1994). Electrooptical device based on polymer-dispersed liquid crystal films. *Jpn. J. Appl. Phys.*, *33*, 1088.

[6] Domash, L. H., Schwartz, J., Nelson, A., & Levin, P. (1992). Active holographic interconnects for interfacing volume storage. *Proc. SPIE*, *1662*.

[7] Tondiglia, V. P., Natarajan, L. V., Sutherland, R. L., Bunning, T. J., & Adams, W. W. (1995). Volume holographic image storage and electro-optical readout in a polymer-dispersed liquid-crystal film. *Opt. Lett.*, *20*, 1325.

[8] Fuh, A. Y.-G., Tsai, M.-S., Huang, C.-J., & Liu, T.-C. (1999). Optically switchable gratings based on polymer-dispersed liquid crystal films doped with a guest-host dye. *Appl. Phys. Lett.*, *74*, 2572.

[9] Doane, J. W., Vaz, N. A., Wu, B.-G., & Zumer, S. (1986). Field controlled light scattering from nematic microdroplets. *Appl. Phys. Lett.*, *48*, 269.

[10] Crawford, G. P., Fiske, T. G., & Silverstein, L. D. (1996). Reflective color displays based on PSCT and H-PDLC technologies. *SID Digest of Technical Papers*, *XXVII*, 99.

[11] Caputo, R., De Sio, L., Veltri, A., Umeton, C., & Sukhov, A. V. (2006). POLICRYPS switchable holographic grating: A promising grating electro optical pixel for high resolution display application. *J. Display Technol.*, *2*, 38–51.

[12] Fuh, A. Y.-G., Lee, C.-R., Liao, C.-C., Shyu, K.-J., Liu, P.-M., & Lo, K.-J. (2001). Dynamic studies of two-beam coupling on the holographic gratings based on liquid crystal–polymer composite films. *Opt. Communications*, *187*, 193.

[13] Bowley, C. C., Smuk, A., Crawford, G. P., & Lawandy, N. M. (2001). Two wave mixing in holographic polymer dispersed liquid crystal (H-PDLC) formation. *Mol. Cryst. and Liq. Cryst.*, *358*, 185.

[14] Caputo, R., De Sio, L., Veltri, A., Umeton, C., & Sukhov, A. V. (2005). Observation of two-wave coupling during the formation of POLICRYPS diffraction gratings. *Opt. Lett.*, *30*, 1840.

[15] Gaylord, T. K. & Moharam, M. G. (1981). Thin and thick gratings: Terminology clarification. *Appl. Opt.*, *20*, 3271.

[16] Veltri, A., Caputo, R., Sukhov, A. V., & Umeton, C. (2004). Model for the photoinduced formation of diffraction gratings in liquid-crystalline composite materials. *Appl. Phys. Lett.*, *84*, 3492.

[17] Caputo, R., De Sio, L., Veltri, A., & Umeton, C. (2005). Model for two beam coupling during the formation of holographic gratings with a nematic film-polymer-slice sequence structure. *Appl. Phys. Lett.*, *87*, 141108.

[18] Caputo, R., Sukhov, A. V., Tabiryan, N. V., Umeton, C., & Ushakov, R. F. (2001). Mass transfer processes induced by inhomogeneous photo-polymerization in a multycomponent medium. *Chem. Phys.*, *271*, 323.